Netherlands Journal of Geosciences — Geologie en Mijnbouw |95 – 3 | 315–335 | 2016 doi:10.1017/njg.2016.23

First assessment of the pore water composition of Rupel Clay in the Netherlands and the characterisation of its reactive solids

Thilo Behrends[1,*], Iris van der Veen[1], Alwina Hoving[1] & Jasper Griffioen[2,3]

[1] Department of Earth Sciences, Utrecht University, P.O. Box 80021, NL-3508 TA Utrecht, The Netherlands
[2] Copernicus Institute of Sustainable Development, Utrecht University, P.O. Box 80115, NL-3508 TC Utrecht, The Netherlands
[3] TNO – Geological Survey of the Netherlands, P.O. Box 80015, NL-3508 TA Utrecht, The Netherlands
[*] Corresponding author. Email: t.behrends@uu.nl

Manuscript received: 15 January 2016, accepted: 13 June 2016

Abstract

The Rupel Clay member in the Netherlands largely corresponds to the Boom Formation in Belgium, and this marine, clay-rich deposit is a potential candidate to host radioactive waste disposal facilities. Prediction of the speciation of radionuclides in Rupel Clay pore water and their retardation by interactions with Rupel Clay components requires knowledge about the composition of Rupel Clay pore water, the inventory of reactive solids and understanding of interactions between Rupel Clay and pore water. Here, we studied Rupel Clay material which was obtained from cores collected in the province of Zeeland, the Netherlands, and from drilling cuttings retrieved from a drilling in the province of Limburg, the Netherlands. Pore water was obtained by mechanical squeezing of Rupel Clay material from Zeeland. Additionally, anaerobic dilution experiments were performed in which the clay material was suspended with demineralised water or a 0.1 M $NaHCO_3$ solution. Solid-phase characterisation included determination of carbon, nitrogen and sulphur contents, measurement of cation exchange capacity (CEC) and sequential extraction of iron phases.

In contrast to the pore water in Belgian Boom Clay, pore water collected from the location in Zeeland has a higher salinity, with chloride concentrations corresponding to 70–96% of those in seawater. The high chloride concentrations most likely result from the intrusion of ions from saline waters above the Rupel Clay in Zeeland. Cation exchange during salinisation might account for the observed deficit of marine cations (Na, K, Mg) and excess of Ca concentrations, in comparison with seawater. The measured CEC values at both locations in the Netherlands vary between 7 and 35 meq $(100\,g)^{-1}$ and are, for most samples, in the range reported for Boom Clay in Belgium (7–30 meq $(100\,g)^{-1}$).

Pore water and solid-phase composition indicate that Rupel Clay from Zeeland has been affected by oxidation of pyrite or other Fe(II)-containing solids. When coupled to the dissolution of calcium carbonates, oxidation of pyrite can account for the elevated sulphate and calcium concentrations measured in some of the pore waters. The relatively low concentrations of pyrite, organic carbon and calcite in the Rupel Clay in Zeeland, in comparison to Limburg, might be an indicator for an oxidation event. Higher contents of dithionite-extractable Fe in Rupel Clay in Zeeland (0.7–2.6 mg Fe / g clay) than in Limburg (0.4–0.5 mg Fe / g clay) might also be a consequence of the oxidation of Fe(II) minerals. Oxidation in the past could have accompanied partial erosion of Rupel Clay in Zeeland before deposition of the Breda Formation. However, indications are given that oxidation occurred in some of the pore waters after sampling and that partial oxidation of the cores during storage cannot be excluded. Results from dilution experiments substantiate the influence of equilibration with calcium carbonates on pore water composition. Furthermore, removal of dissolved sulphate upon interaction with Rupel Clay has been observed in some dilution experiments, possibly involving microbial sulphate reduction.

Keywords: cation exchange capacity, pore water, reactive iron minerals, Rupel Clay, sequential extraction

Introduction

Clay-rich sedimentary deposits are potential candidates to host radioactive waste disposal facilities due to the low permeability of clay and the capability of clays to retard radionuclide migration due to interactions between radionuclides and the solid phase. Performance assessment of a disposal facility for radioactive waste requires quantitative predictions about the ability of

the surrounding geological formation to retard the transport of radionuclides. Mobility of radionuclides in the host formation depends, among other factors, on their speciation and the interactions of the radionuclide species with the solids. Hence, constraining the composition of *in situ* pore water as well as the characterisation and quantification of reactive solids in the geological formation hosting the disposal facility containing radioactive waste is a prerequisite for predicting the interaction of radionuclides with the host rock. Knowledge of the pore water composition of the host rock is also of pivotal importance for assessing the evolution of the engineered barrier system, corrosion of its metallic components, and the prediction of the source term of different waste forms regarding the release of radionuclides.

Boom Clay has been studied as the reference host formation for the geological disposal of radioactive waste in Belgium, and its mineralogy and the composition of *in situ* pore water has been extensively investigated and reported in publications and reports (Vandenberghe, 1974, 1978; Decleer et al., 1983; Laenen, 1997; De Craen et al., 2004, 2006; Honty and De Craen, 2009, 2012; Zeelmaekers, 2011). The characteristics of Boom Clay in Belgium are well known because Boom Clay outcrops are accessible in various clay pits. Furthermore, the Hades underground research facility in Mol offers access to Boom Clay material and unique opportunities to determine *in situ* pore water composition by using piezometers. An equilibrium model was used to reproduce the compositions of pore waters retrieved from the MORPHEUS piezometer in Mol, Belgium (De Craen et al., 2004). In this model, the CO_2 pressure and the sulphate concentration was constrained and the solution was equilibrated with the cation exchange complex and the following minerals: chalcedony, kaolinite, calcite, siderite and pyrite. This model does not include other mineralogical components with lower reactivity such as quartz, K-feldspars, albite, and heavy minerals such as illmenite, rutile, anatase, xenotime, monazite or zircon, which have been detected in Boom Clay (De Craen et al., 2004). In general, Fe-containing minerals are important for the migration of radionuclides as some of them, such as pyrite, can reduce or oxidise redox-sensitive radionuclides and/or have a high sorption capacity and affinity for radionuclides. An important group of reactive Fe solids, which are particularly relevant in soils, are iron (oxyhydr)oxides. However, the presence of iron or aluminium (oxyhydr)oxides in Boom Clay has not been reported so far.

In the Netherlands, the Rupel Formation according to the Belgian nomenclature is equivalent to the part of the Rupel Clay Member that overlies the upper part of the sandy Vessem Member of the Rupel Formation. In contrast to Boom Clay in Belgium, little is known about the characteristics of Rupel Clay in the Netherlands. Koenen and Griffioen (2016) investigated Rupel Clay samples from 17 different cores from various locations in the Netherlands. They found, based on statistical analysis of chemical and mineralogical data, that three regional variations of Rupel Clay can be distinguished: Rupel Clay in the north of the Netherlands is more homogeneous and has a higher clay content than Rupel Clay in the south; Rupel Clay from the southeast is different to that from the southwest due to its higher carbonate content.

Material from Rupel Clay in the Netherlands has been geochemically characterised and reported as part of the Dutch research programmes CORA and OPERA (Rijkers et al. 1998; Koenen and Griffioen, 2013, 2016). To our knowledge, all analyses so far have been performed on core material which was stored without specific precautions to prevent alterations due to oxidation by atmospheric oxygen or desiccation. These two processes might change the composition and mineralogy of the material. Possible reactions include the oxidation of organic matter or of redox-sensitive solids such as pyrite (FeS_2) or siderite ($FeCO_3$). The oxidation of pyrite can lead to the formation of iron (oxyhydr)oxides and the generation of sulphuric acid, which in turn can further react with carbonates and eventually result, for example, in the precipitation of gypsum ($CaSO_4{\cdot}2H_2O$) or jarosite ($KFe_3(OH)_6(SO_4)_2$). Indications for secondary gypsum formation were obtained from the inspection of Rupel Clay material from the TNO core house (Koenen and Griffioen, 2013). Dissolved ions can form precipitates upon the evaporation of water, while the amount of dissolved ions can be altered during the concentration process due to the interactions with the solid phase including ion exchange and other sorption processes. Hence, material from these cores is only suitable for the determination of parameters which are not, or only marginally, susceptible to alteration upon oxidation and drying. These parameters include the mineralogy of less reactive minerals (e.g. silicates), total element content, or particle size. For the determination of reactive solid phases or the analysis of pore water composition, fresh or carefully preserved cores are required.

To our knowledge, no attempt has yet been made to retrieve *in situ* pore water, or to reconstruct *in situ* pore water composition, of Rupel Clay in the Netherlands. In view of pore water composition, salinities up to 24 g L^{-1} have been reported from Rupel Clay at a location in Zeeland (Rijkers et al., 1998). These high salinities were attributed to an influence of water from the Scheldt estuary. Deep groundwater in the Netherlands often contains high salt concentrations (Griffioen 2015; Griffioen et al., 2016). Deep groundwater below the Rupel Clay is generally saline or hypersaline. Water with higher salt concentrations than seawater occurs in groundwater below the Rupel Clay in the north of the Netherlands and is most likely a consequence of the dissolution of evaporite deposits. Elevated chloride concentrations in groundwater above the Rupel Clay, reaching up to seawater levels, are also encountered in the Netherlands, most frequently in the northern Netherlands. This suggests that electrolyte-rich water in the vicinity of Rupel Clay can influence the composition of its pore water in the Netherlands and that Rupel Clay pore water in the Netherlands

might often have higher electrolyte concentrations than in Belgium.

Here, we characterise Rupel Clay material from two different locations in the Netherlands. The investigated material was either obtained from cores which were stored in wax sealed stainless steel cylinders in order to optimise preservation after core collection or from core cuttings which were preserved against drying and oxidation directly after collection. The aim is to investigate the presence and quantity of reactive constituents, and related parameters such as cation exchange capacity, of Rupel Clay material from the Netherlands. Furthermore, attempts are made to retrieve pore water and to reconstruct the *in situ* pore water composition. The results are compared with those obtained from unaltered material in Belgium in order to evaluate possible regional differences and identify processes which have caused these differences.

Sampling location and sample treatment

Rupel Clay material was obtained from two locations in the Netherlands: cores were selected from five drillings close to Borssele village in the province of Zeeland (Fig. S1 in Supplementary Material), and core cuttings were retrieved from a geothermal drilling close to Grubbenvorst, located in the province of Limburg. For this study, samples from three core sections collected from three of the five different drillings in Zeeland were investigated. At the location in Zeeland, the Rupel Clay strike-line runs approximately NW–SE and is dipping towards SW. In the different drillings in Zeeland which were used in this study, the top of Rupel Clay is found at a depth interval between 63 and 70 m below sea level. The thickness of the Rupel Clay in the drillings varies between approximately 10 and 18 m. According to the digital geological model of the Netherlands (TNO, n.d.), the basis of the Rupel Clay proceeds evenly along the striking and dipping lines, while the morphology of the upper boundary is undulating (Fig. S2 in Supplementary Material). The Breda Formation is part of the Upper North Sea Group, which overlies disconformably or unconformably the Middle North Sea Group (TNO, 2003). The Rupel Clay is the top layer of the Middle North Sea Group at the location in Zeeland, and the Veldhoven formation is missing. Hence, the variation of the Rupel Clay thickness and the undulating boundary between Rupel Clay and the Breda Formation may be a consequence of partial erosion of the Rupel Clay before the Breda Formation was deposited. At Grubbenvorst, the Rupel Clay has a thickness of about 100 m and was encountered during the drilling at a depth interval between about 530 and 630 m below surface. During the drilling in Grubbenvorst, Rupel Clay samples were collected upon about each 5 m of drilling progress.

The cores from Zeeland were collected in June 2011, and cores were preserved in Shelby tubes which were sealed with paraffin wax at the top and bottom. Remaining void space was filled with clean sand, and the tubes were closed with a plastic cap wrapped with PVC tape. In November 2012, the cores were opened and sliced. For subsampling the core, the steel cylinder was cut on both sides with an angular grinder. To avoid heating of the core the location of the grinder was frequently changed and only applied for short moments at one spot. The core was removed and transferred into a glove box with N_2/H_2 95%/5% atmosphere. When removed from the Shelby tubes, it appeared that the surfaces of the cores were covered with a thin brown layer, indicating that iron (hydr)oxides had formed upon the reaction with atmospheric oxygen (Fig. S3 in Supplementary Material). These layers were removed prior to cutting and subsampling. The core was subsequently sliced in 2 cm thick horizontal layers numbered from top to bottom. The slices were individually installed in bags consisting of an aluminium layer between two plastic (polypropylene and polyethylene) layers (PP/Al/PE) which were heat-sealed inside the glove box and stored at 4°C until usage.

The structure of the material in the core was not homogeneous. Clay-rich layers with high plasticity alternated with layers with brittle structure and lower clay content. The coloration of these brittle sections varied between white, grey and dark brown. The occurrence of brownish patches in the interior of the core indicates that this material has been affected by oxidation (Fig. S3 in Supplementary Material). Oxidation inside the core could have happened during storage by intrusion of oxygen through larger pores or fractures by the atmospheric oxygen which entered void space in the cores during sealing or by oxygen which entered the core by diffusion through the plastic caps during storage. Larger pores might have been present in sections with lower content of fine material. Clay-rich parts exhibited a grey colour and did not show indications for oxidation inside the core based on visual inspection.

In order to account for the diversity of structure and composition, slices were selected based on visual inspection which are representative for different core features encountered during slicing (Table 1, and Table S1 in Supplementary Material). Aliquots from the slices presented in Table S1 were used in the dilution experiments and subjected to geochemical characterisation. The geochemical characterisation also included aliquots of other slices and four samples from Grubbenvorst (Limburg).

Core cuttings were retrieved in August 2012 and were captured from the outflow at the drilling rig using a sieve. They were then rinsed with demineralised water to remove drilling fluids, and put into PE bags. The PE bags were stored in a glass jar which contained Anaerocult® A bags to remove oxygen and to prevent reaction with atmospheric oxygen during transport into the laboratory. In the laboratory, the samples were transferred inside the glove box into PP/Al/PE bags which were heat-sealed inside the glove box and stored at 4°C until usage.

Table 1. Slices from the different core sections used in this study and the corresponding depth. The number after the hyphen in the name of the Zeeland samples indicates the number of the 2 cm slice sampled from top to bottom.

Sample name	Depth (m)	Approximate distance (m) from Rupel Clay top
Zee 101–14	72.64	3.5
Zee 101–24	72.84	3.5
Zee 103A-01	78.72	8.5
Zee 103A-19a	79.10	8.5
Zee 103A-19b	79.10	8.5
Zee 103A-22	79.16	8.5
Zee 104–10	75.56	2
Zee 104–24	75.76	2
Limburg 2	525	
Limburg 9	570	
Limburg 5	595	
Limburg 19	620	

Methods

Pore water collection by mechanical squeezing

Pore water was collected by mechanical squeezing of Rupel Clay material. The required sample preparation and the squeezing of the sample was performed at SCK-CEN in Mol, Belgium, according to the method described by De Craen et al. (2004). The composition of the solution obtained from mechanical squeezing could deviate from the free, *in situ* pore water due to a variety of processes including: forcing out adsorbed water at high pressures, filtration and membrane effects, and perturbation of thermodynamic equilibria at elevated pressure (Fernández et al., 2013). For Boom Clay, solutions obtained by mechanical squeezing were found to be representative for the *in situ* pore water collected in piezometers with a YM3 filter (De Craen et al., 2004). In the following, it is therefore assumed that the composition of pore water has not been altered upon squeezing itself and represents free pore water. Free water excludes water which is surface-sorbed or is part of the diffuse layer surrounding charged surfaces and, in a first approximation, can be conceived as the water in the anion-accessible pore volume (Fernández et al., 2013). This does not exclude the possibility that chemical reactions can change the composition of the retrieved solution after the solution has been collected in a sampling bottle. About 700 g of Rupel Clay material was loaded inside a steel cylinder which was closed at the top with a piston. The loading of the cell with the sample was performed inside a glove box under nitrogen atmosphere to prevent exposure of the sample to atmospheric oxygen. A porous steel plate at the bottom of the cylinder allowed pore water to leave the cylinder when a pressure of 30 MPa was applied to compress the sample. The pressure was applied over one week while pore water was being collected. The pore water left the cylinder through a steel capillary and was collected in a N_2-gas-containing serum bottle which was sealed and equipped with a water-filled airlock to allow escape of nitrogen from the bottle and to prevent intrusion of atmospheric oxygen. For the extraction of the first two samples, Zee 101 and Zee 104, the flask was closed with a straight, grey butyl stopper. After analysis of the retrieved solution, suspicion arose that oxygen might have leaked through these stoppers and might have reacted with dissolved Fe(II), S(-II) or nanoparticulate FeS in the squeezed pore water. For this reason, a thick black rubber stopper was used during the third extraction of Zee 103 material. The squeezing of about 700 g clay material yielded about 40–50 mL of pore water. Afterwards, the remaining water content of the clay was determined by measuring the weight loss of the sample upon drying at 105°C.

Dilution experiments

An alternative approach to assess the *in situ* composition of the pore water is to suspend clay-rich sediments in demineralised water or bicarbonate solution (De Craen et al., 2004). Two strategies can be followed to obtain information about the *in situ* pore water composition by dilution experiments: (1) After suspending the clay, the liquid phase is separated as soon as possible from the suspension. If the duration of suspending the material and the subsequent separation of the solution is significantly shorter than the time scale of reactions between the solution and the suspended solids, the composition of the solution reflects, in the first instance, the dilution of the *in situ* pore water. (2) The contact time of the solution with the clay material is sufficiently long to reach equilibrium. The composition of the solution then reflects the concentrations of those solutes whose concentrations are *in situ* controlled by equilibrium reactions between solution and the solid phase. In practice, neither of these idealised situations is usually fulfilled. This is because some heterogeneous reactions occur very fast, such as adsorption, desorption or evasion of gases, while others proceed so slowly that equilibrium cannot be reached during a laboratory experiment at room temperature. These slow processes include dissolution or precipitation of minerals or redox transformations. Hence, the composition of the retrieved solutions after dilution has to be carefully interpreted when assessing the *in situ* pore water composition. In order to obtain information about the potential role of mineral–water interactions in controlling the composition of the extracted solution after dilution, experiments were performed in three different solid-to-solution ratios and solution was retrieved after four different reaction times.

Table 2. Composition of the different dilution experiments and the corresponding solid-to-solution ratios.

Solid to solution ratio ($g\,L^{-1}$)	Clay sample amount (g)	Solution volume (mL)
25	1.25	50
50	2.50	50
200	8.00	40

When the solution composition is solely controlled by dilution of the *in situ* pore water, the composition of the latter can be determined based on the dependency of the concentrations in the diluted solutions (C in $mol\,L^{-1}$) on the ratio of the volume of the added solution to the mass of clay material (V_{added}/m_{solid} in $L\,g^{-1}$):

$$\frac{1}{C} = \frac{V_{pore}}{n_{pore}} + \frac{m_{solid}}{n_{pore}} \cdot \frac{V_{added}}{m_{solid}}$$

wherein V_{pore} is the total volume of non-adsorbed water in the clay in litres and n_{pore} is the total amount of the constituent initially present in the *in situ* pore water in mol. The latter implies that n_{pore}/V_{pore} represents the average concentration of solutes in the Rupel Clay water and is based on the assumption that the clay is completely suspended. In this case, anion exclusion in small pores does not occur, implying that n_{pore}/V_{pore} might underestimate the concentration of anions in the anion-accessible pore volume of the Ruppel Clay. For example in Opalinus Clay, anions might be excluded from roughly 30–50% of the total pore volume (Fernandez et al., 2013). However, with increasing ionic strength, the exclusion effect is expected to become smaller (Tournassat and Steefel, 2015). When dilution is the dominant factor controlling the solution composition, 1/C depends linearly on V_{added}/m_{solid}. The slope of the line, obtained by linear regression analysis, then gives m_{solid}/n_{added}. The concentration of the constituent in the pore water could be directly obtained from the intercept of the regression line with the y-axis. However, the uncertainty of the intercept is typically large. For this reason, the concentration of the pore water was calculated by dividing n_{added}/m_{solid}, the reciprocal value of the slope, by V_{pore}/m_{solid}, the pore water volume of the sample. The latter was determined independently from the weight loss upon freeze-drying. Pore water concentrations were only reported from the dilution method when the coefficient of determination of the regression line, r^2, was larger than 0.95.

For the dilution experiments, Rupel Clay material was ground and homogenised inside the glove box, added into 50 mL PP centrifuge tubes and mixed with 0.01 M $NaHCO_3$ solution or demineralised water in three different solid-to-solution ratios (Table 2). Prior to addition, the pH of the $NaHCO_3$ solution was adjusted to 8.12. This solution is in equilibrium with a CO_2 pressure of about 403 Pa, which has been reported for Boom Clay in Mol, Belgium (De Craen et al., 2004). The preparation of the suspensions and the collection of samples were performed in a glove box with a N_2/H_2 95%/5% atmosphere. The contact time of the solution with the glove box atmosphere was kept as short as possible and the headspace within the centrifuge tubes was small so that the effect of CO_2 outgassing on the dissolved inorganic carbon (DIC) concentration content and the pH of the solution should be insignificant. After the preparation of the suspensions, the centrifuge tubes were installed in a glass jar with a rubber sealing ring as an additional protection against the intrusion of atmospheric oxygen. The glass jars were then removed from the glove box and placed on a temperature-controlled horizontal shaker, on which the suspensions were constantly agitated at 26°C, implying that equilibrium state of solid–solution reactions could be different to that under *in situ* conditions (roughly 10°C) and abiotic reactions could proceed faster than under *in situ* conditions. All dilution experiments were performed in duplicate.

For sampling the solution, the glass jars were transferred back into the glove box and an aliquot of the suspension was removed and added into a 15 mL PP centrifuge tube. The remaining suspension was returned into the glass jar and placed back on the shaker. The pH was determined in the aliquots, and 0.5 mL of the suspension was kept for TXRF analysis. The remaining aliquots were centrifuged for 1 hour at 2700 g. After transferring back into the glove box, the supernatant was carefully decanted and filtered through a syringe filter with a 0.2 μm pore size nylon membrane. One millilitre of the filtered solution was acidified with 100 μL 0.2% HNO_3 for inductively coupled plasma optical emission spectrometry (ICP-OES) analysis, and the remaining solution was kept for other analyses.

Sequential extractions

Due to the potential importance of Fe minerals for radionuclide migration, a sequential extraction of different Fe phases was carried out according to the modified procedure developed by Claff et al. (2010) (Table 3). The extraction consists of six steps targeting exchangeable Fe, Fe carbonates and minerals sensitive to low pH, Fe bound to organic matter, crystalline Fe oxides, pyrite and the residual Fe fraction, respectively. Extractions were performed with 1 g of sample, and in the first five steps 40 mL of the various extraction solutions was added. The sequential extractions were performed in triplicate. The first three extraction steps were carried out inside a glove box under a N_2/H_2 atmosphere. The last three steps were performed outside the glove box.

For the aqua regia extraction, the sediment samples were dried overnight in an oven at 75°C after being transferred into Teflon® reaction vessels. After drying, 1.5 mL of concentrated HNO_3 and 4.5 mL of concentrated HCl (aqua regia) was added to the sample and reacted at 90°C overnight within the closed vessels. The following day, the vessels were opened and fluids were

Table 3. Modified extraction scheme according to Claff et al. (2010).

Extraction step	Extractant	Phase extracted	Source
1	1 M magnesium chloride ($MgCl_2$) at pH 7, extracted for 1 hour	Exchangeable fraction of adsorbed Fe and readily soluble Fe-salts	Tessier (1979)
2	1 M hydrochloric acid (HCl), extracted for 4 hours	Carbonates and other minerals sensitive to low pH	Larner (2006); Scouller (2006)
3	0.1 M sodium pyrophosphate ($Na_4P_2O_7$) at pH 10.4, extracted for 16 hours	Iron bound to organic matter	Donisa (2007)
4	Sodium citrate/dithionite solution buffered to a pH of 7.5 with $NaHCO_3$ (CDB), extracted for 15 minutes in a water bath at 75°C.	Crystalline iron oxides	Gleyzes (2002)
5	Concentrated nitric acid (HNO_3), extracted for 2 hours	Pyrite	Huerta Diaz (1990)
6	Aqua regia	Residual fraction of solid bound Fe	Mossop (2003)

evaporated at 160°C. After evaporation, 20 mL of 2% HNO_3 was added to the dried residuals and reacted for 12 hours at 90°C. Afterwards, the remaining amount of 2% HNO_3 was determined by weighing and the solution was analysed with ICP-OES. Additionally, an aqua regia extraction was performed with Rupel Clay material which has not undergone the previous extraction steps. As a quality indicator, the sum of the extracted Fe during the various steps was compared to the Fe recovered in the independent aqua regia extraction.

Between the steps of the sequential extraction, the samples were centrifuged at 2800 g for 10 minutes. The supernatant was decanted into a 50 mL Greiner tube and diluted 1 : 10 with 2% HNO_3 prior to ICP-OES analyses. After the concentrated HNO_3 step, the solution was diluted with demineralised water. After the extraction steps 1, 2, 3 and 5, the solids were resuspended with $MgCl_2$ solution, centrifuged again at 2700 g for 1 hour, and the washing solution was decanted. $MgCl_2$ solution was used instead of demineralised water as, otherwise, clay particles remained in suspension after centrifugation. After step 4, the sediment was rinsed with the dithionite/citrate/bicarbonate (DCB) extraction solution. All the extraction steps were carried out at room temperature, except for step 4, which was carried out in a water bath of 75°C, and aqua regia extraction was performed at 90°C.

Cation exchange capacity

Two different methods were used to determine the cation exchange capacity (CEC): the Ag-thiourea method (Dohrmann, 2006) and the Cu(II)-triethylenetetramine (Cu-trien) method (Ammann, 2005; Honty, 2010). The Cu(II)-triethylenetetramine has been recommended as a standard method for CEC measurements in Boom Clay (Honty, 2010). The Ag-thiourea method was selected as an efficient, alternative method for determining CEC in clays (Dohrmann, 2006), but, due to problems related to the precipitation of elemental Ag during the application of the Ag-thiourea method, only results from using the Cu-trien method are reported.

The Cu-trien solution was prepared by dissolving 1.49 mL of triethylenetetramine in 100 mL of demineralised water, adding 1.596 g of $CuSO_4$ and demineralised water until a final volume of 1 L was reached. Forty millilitres of DI water were added to 200 mg of sediment, after which 10 mL of the Cu-trien solution was added. The samples were sonicated for 15 minutes to suspend the clay material. After sonication, the sediments were shaken for 30 minutes at 120 rpm. The samples were centrifuged at 2680 g, after which the supernatant was decanted, and analysed with ICP-OES. Additionally, Cu concentrations were measured by spectrophotometry at 577 nm (Ammann, 2005). The difference in Cu concentration before and after the reaction with the sediment samples was used to calculate the amount of adsorbed Cu and, by this, the CEC. All samples were analysed in triplicate.

Analytical procedures

C, N, S content Contents of C and S were determined before decalcification with a LECO SC632 carbon/sulphur analyser. The samples were combusted under an oxygen flow at ±1350°C and C and S were measured as CO_2 and SO_2 with infrared detectors. The gas flows for purging and during measurement were adjusted to $2.5 \pm 0.1\ L\ min^{-1}$. Additionally, C and N contents were determined after decalcification. For decalcification, 0.3 g of the ground and freeze-dried sample was added into a 15 mL PP centrifuge tube and 7.5 mL of 1 M HCl was added. After the sample had stopped bubbling, tubes were closed and shaken for 12 hours. The supernatant was decanted after centrifugation at 2100 g for five minutes. Acid addition was repeated with a shorter reaction time of four hours. After removal of the acid, the solid was washed with demineralised water in two cycles of resuspension and centrifugation. Finally, the C and N contents were determined with a carbon/nitrogen analyser in which the

Table 4. Chemical composition of solution retrieved by mechanical squeezing from core Zee 101 (slices 17 and 18), Zee 104 (slices 9 and 11) and Zee 103 (slices 11–13). The reported uncertainties indicate the variation between duplicate measurements. Evaluation of the calibration with independent standards was in the range ±5%. Measured concentrations are compared to those reported for Boom Clay pore water in Mol (De Craen et al., 2004) and in Essen (De Craen et al., 2006). The groundwater composition of the Breda Formation was taken from data reported for the well B48G0059 which has a well screen 50.9–51.9 m below surface. The well is located close to Oudelande, about 7 km ESE of the location in Zeeland where the Rupel Clay samples were collected. The well was sampled on 27 October 1988. Data from the well B48G0204, which is located close to well B48G0059, were used for the composition for the groundwater in the Tongeren Formation. The well has a well screen 124–142 m below the surface and the average of data from sample collection on 1 January 2006 and 18 December 2007 is given. For comparison, the seawater composition according to Appelo and Postma (2005) is also listed.

	Seawater	Zee 104	Zee 101	Zee 103	BC in Mol, Belgium	BC in Essen, Belgium	GW Breda Formation	GW Tongeren Formation
Na (mM)	485	443[a] ± 3	237[a] ± 4	133.1 ± 0.1	15.6	56	317	19.6
Cl (mM)	566	546[a] ± 2	408[a] ± 5	394.0 ± 0.1	0.5	44.1	450	13.8
S (mM)	29	65[a] ± 2	57[a] ± 1	3.9 ± 0.1	0.02[b]	4.2[b]	3.2[b]	0.25[b]
K (mM)	11	15.95[a] ± 0.02	10.4 ± 0.2	3.7 ± 0.2	0.2	0.7	8.1	0.63
Ca (mM)	11	47.0 ± 0.1	60.4 ± 0.7	69.7 ± 0.1	0.04–0.2	0.9	35.7	0.35
Mg (mM)	55	51.7 ± 0.3	42.3 ± 0.5	58.4 ± 0.1	0.05–0.2	2	32.3	0.58
Fe (μM)		297 ± 1	746 ± 12	3260 ± 0.1	6–50	70	163	
pH	7.5–8.4	3.05	3.17	6.7	8.3–8.6	8.3–8.6	6.26	8.27
Alkal. (mEq)	2.47			0.55			5.0	
I[c] (mM)		830	649	529				
IB[d] (mEq)		−20	−68	−9				
IB/I (%)		−2.4	−10	−1.7				

[a]Concentrations exceeded the calibration range and might have an error > 5%; [b]SO_4^{2-} concentration; [c]ionic strength; [d]ion balance.

sample is combusted and the combustion gases are reduced over a Cu column, separated by gas chromatography and detected with a thermal conductivity detector.

Analysing aqueous solutions The elemental composition of solutions was determined by ICP-OES. Alkalinity was determined by titration with 0.1 M HCl and analysing the titration curve with the Gran method. A standard combined glass electrode with temperature sensor was used to determine pH. DIC concentrations were determined using a Shimadzu TOC 5050 analyser.

For redox-specific determination of Fe(II) and Fe(III) a modified ferrozine method was applied (Viollier et al., 2000). In brief, to 1.2 mL of the aqueous sample, 200 μL of 0.01 M ferrozine reagent (monosodium salt hydrate of 3-(2-pyridyl)-5-6-bis (4-phenylsulphonic acid)- 1,2,4 triazine p-p'-disulphonice acid) was added plus 300 μL of demineralised water and 200 μL of 5 M ammonium acetate buffer with a pH of 9.5. The mixture was stirred and the absorbance was measured in polystyrene cuvettes at 562 nm with a photospectrometer. For determining total Fe, 300 μL of 1.4 M hydroxylamine in 2 M HCl was added instead of demineralised water. In this case the buffer solution was added after 10 minutes' reaction time and the formed Fe(II) was determined as described above.

TXRF Total reflection X-ray fluorescence (TXRF) was used to determine the Cu content of the sediment sample after the CEC determination. TXRF measurements were performed with a Bruker S2 Picofox. Five hundred milligrams of sample were dispersed in 10 mL of 1% Triton-X solution. One hundred microlitres of 250 ppm Ga solution were added as internal standard to the suspension. Five microlitres of the suspension were pipetted on a glass slide and analysed with TXRF.

Thermodynamic equilibrium calculations

The equilibrium speciation of solutions was calculated using PHREEQC for Windows (Parkhurst and Appelo, 2013). Calculations were performed for a temperature of 298 K, and the WATEQ4F or Pitzer database, obtained as part of the standard installation of PHREEQC, was used.

Results and Discussion

Pore water obtained by mechanical squeezing

The pore waters are saline, with ionic strengths (I) ranging between 0.53 and 0.83 M (Table 4). All ion balances (IBs) are negative, but the ratio IB/I is in the range which can be explained by analytical error. Systematically negative ion balances could indicate the presence of cations with millimolar concentrations which are not listed in the table. Chloride concentrations in the retrieved pore waters from the three cores range between 70 and 96% of the chloride concentration in seawater and decrease with increasing distance to the Rupel Clay top. The Cl concentrations

Table 5. Chemical composition of the in situ pore water calculated from the concentrations in the solutions retrieved from the dilution experiments after about three hours' reaction time.

	10 mM $NaHCO_3$					Demineralised water		
	Zee 101–14	Zee 103A-01	Zee 103A-19a	Zee 103A-19b	Zee 103A-22	Zee 101–14	Zee 103A-19a	Zee 103A-22
Na (mM)	[a]	[a]	[a]	[a]	[a]	389	368	330
Cl (mM)	500	213	410	464	424	584	429	465
S (mM)	94.6	61.8	12.5	ND	ND	106	72	ND
K (mM)	90.4	261	74.5	124	34	57.2	50.0	33.4
Ca (mM)	53.6	ND	45.8	53.6	45.2	26.9	28.5	38.8
Mg (mM)	36.5	2.50	31.2	35.8	31.5	19.5	21.4	22.4
pH[b]	7.6	10.5	7.6	7.3	7.7	7.4	7.4	8.2
I (mM)						820	667	550
IB (mEq)						−257	−55	8
IB/I (%)						−31	−8.3	1.5

[a]Due to high Na concentrations in the added solution, the Na concentrations in the in-situ pore water could not be calculated. ND = not determined because $r^2 < 0.95$. [b]The pH value is the average value of all different dilutions and replicates.

are comparable to those in the groundwater of the Breda Formation which overlies the Rupel Clay at the location in Zeeland (Table 4). In contrast, the Cl concentrations in groundwater of the Tongeren Formation below the Rupel Clay are about 40 times lower than in seawater (Table 4). The presented data are from an aquifer in the lower part of the Tongeren Formation, the Layer of Bassvelde, which is separated from the Rupel Clay by another clay-rich layer. However, data from another well in the vicinity (B54E0269) indicate that the chloride concentrations of the groundwater directly below the Rupel Clay are about 9 mM. Hence, at the location in Zeeland, the Rupel Clay separates groundwater with saline signature from groundwater with slightly brackish character. As a consequence, the seawater influence on the pore water composition of Rupel Clay in Zeeland is significantly higher than in Mol or Essen, Belgium. Also the concentrations of other major cations and anions in the retrieved pore water from the samples in Zeeland are, in general, one or two orders of magnitude higher than in the Boom Clay in Belgium at the locations Mol or Essen (Table 5). When taking the Cl concentrations as a reference, the pore water of Rupel Clay in Zeeland is relatively enriched in Ca and for samples Zee 101 and Zee 104 also in S. In contrast, sample Zee 103 is relatively depleted in S with respect to seawater. The S concentrations in the latter sample are comparable to those in the overlying groundwater in the Breda Formation. The groundwater is also relatively enriched in Ca and depleted in S with respect to seawater. A depletion in dissolved S can be attributed to microbial sulphate reduction when coupled to the precipitation of sulphides.

The Mg/Cl ratios are similar or moderately higher in the different pore waters compared to seawater, which is also the case for the K/Cl ratios with the exception of the pore water of Zee 103, which has a lower K/Cl ratio than seawater. The solutions from samples Zee 103 and Zee 104 are depleted in Na with respect to seawater, which is reflected in lower Na/Cl ratios. The relative depletion in Na is most pronounced in the groundwater from the deepest part of the Rupel Clay, in sample Zee 103, and the Na/Cl ratios increase towards the top. A shift in cation composition can be explained by cation exchange. For example, Ca can be exchanged against Na when, initially, the cation exchange complex is dominated by Ca and Na enters the sediment either by convective transport or by diffusion. This, in turn, can lead to an increase in Ca/Cl ratios and a decrease in Na/Cl ratios and would provide an explanation for lower Na concentrations and higher Ca concentrations relative to seawater. The base exchange index, BEX = Na + K + Mg – 1.0716 Cl in mEq (Stuyfzand, 2008), is negative for the solutions of all samples. A negative BEX indicates salinisation of an aquifer when the deficit of marine cations is caused by cation exchange. Also in the groundwater of the Breda Formation, the BEX index is negative. This implies that the cation assemblage of the seawater has already been modified by cation exchange during its underground passage before reaching the Rupel Clay. In comparison with the Rupel Clay pore water, the negative BEX value in the Breda groundwater is predominately caused by a depletion of Mg while in the pore waters, particularly in samples Zee 101 and Zee 103, Na concentrations are relatively lowered with respect to seawater.

The effect of cation exchange on pore water composition is particularly expected at the forepart of a progressing salinity front. In a previous COVRA (Central Organisation for Radioactive Waste, the Netherlands) report, Rijkers et al. (1998) presented

a Cl profile in Rupel Clay measured in a core which was retrieved about 9 km southwest of the drillings presented in this study: the salinity in the upper 10–12 m of Rupel Clay was significantly higher than in the lower part of the Rupel Clay. The salinity profile was interpreted as a recent process of a progressing salinity front. The investigated core sections Zee 101 and Zee 103 were located about 4 and 9 m, respectively, below the boundary between Rupel Clay and the Breda Formation. The distance of 9 m corresponds to the progress of the salinity front reported in the COVRA report; hence, the cation composition in the solution in sample Zee 103 might reflect pronounced cation exchange at the forefront of a progressing salinity plume.

In addition to cation exchange, the pore waters of samples Zee 104 and Zee 101 have been altered by pyrite oxidation coupled to carbonate dissolution. When using the Cl concentrations as an indicator for the seawater component in the pore water, the absolute enrichment in S and Ca in the pore water varies between 36 and 53 mM. In sample 104, the enrichment in S and Ca is very similar. This suggests that the pore water composition has, in addition to cation exchange, been influenced by the oxidation of pyrite combined with the dissolution of $CaCO_3$:

$$4FeS_2 + 15O_2 + 10H_2O + (16 - 8x)CaCO_3 \rightarrow (16 - 8x)Ca^{2+}$$
$$+4FeOOH + (16 - 16x)HCO_3^- + 8xH_2CO_3 + 8SO_4^{2-}$$

The equation presents the stoichiometry of the reaction when pyrite oxidation is coupled to the reduction of oxygen. The reaction of pyrite with oxygen generates H^+ which can be neutralised by the dissolution of calcium carbonates. The stoichiometric ratio between the produced Ca and SO_4 varies between 1 : 1 and 2 : 1 depending on carbonate speciation. The variable x in the equation is the fraction of produced H_2CO_3. When virtually all DIC is in the form of bicarbonate (HCO_3^-) (which is the case in a first approximation in the pH range 7.4–9.3), x is approximately zero, resulting in a Ca/SO_4 ratio of 2 : 1. Under acidic conditions (in a first approximation at $pH < 5.3$) carbonic acid (H_2CO_3) is the dominant dissolved carbonate species (x is approximately 1) and the stoichiometric ratio between produced Ca and SO_4 ratio is 1.

The extent of pyrite oxidation in the sample could be larger than inferred from the excess of dissolved Ca and SO_4 with respect to seawater if the solution becomes oversaturated with respect to gypsum and gypsum precipitation is induced. If today's seawater is equilibrated with gypsum, about 22 mmol of gypsum is dissolved per litre, leading to concentrations of Ca and SO_4 of about 33.0 and 50.5 mM, respectively (Holland, 1984). These values are exceeded by the measured concentrations in the collected pore water from samples Zee 101 and Zee 104. Calculated saturation indices for gypsum ranged between 0.27 and 0.42 for the solutions Zee 104 and Zee 101 and were 0.02–0.04 units higher when the WATEQ4F database (based on an ion-association model and using the Davies equation for calculating mean activity coefficients) was used in comparison to the Pitzer database (based on the Pitzer specific interaction approach). Hence, both solutions are supersaturated with respect to gypsum, and precipitation of gypsum could have affected the pore water composition. Furthermore, the oversaturation of the solution might indicate that the elevated Ca and SO_4 concentrations are a result of recent pyrite oxidation and the time since this event has been too short for reaching equilibrium. Growth of gypsum is a relatively fast process and the saturation index of a supersaturated solution containing 0.5 M NaCl decreases from 0.17 to 0.04 in the time scale of a few hours when seed crystals are added (Brandse et al., 1977). In the absence of seeding crystals, the induction period for gypsum nucleation from homogeneous solution can be tens of hours at the determined levels of supersaturation in the pore water (He et al., 1994). Consequently, the observed gypsum supersaturation indicates that the pore water composition has been altered due to pyrite oxidation during storage or during pore water collection, but also the possibility of enhanced SO_4 and Ca release from the sample due to the applied pressure cannot be excluded as gypsum solubility increases with pressure (Blount and Dickson, 1973).

The pH in sample Zee 103 and the alkalinity are lower than in seawater, indicating that part of the acid neutralisation capacity associated with intruding seawater constituents has been consumed. Acidification is more pronounced in the solutions obtained from samples Zee 104 and Zee 101 having an acidic pH value around 3.2–3.0. These values are significantly lower than the pH value of 6.5 in the solution from sample Zee 103 and the pH values reported from Boom Clay pore water at other locations. Most likely, the low pH values of samples 104 and 101 do not reflect the acidity of the *in situ* pore water but acidity has been produced in the solution after it has been squeezed out from the sample. A likely process producing acidity in the sample is the oxidation of dissolved Fe(II), S(-II) or particulate iron sulphides which are small enough to pass the pores of the clay and the porous steel plate. When the contact of the solution with atmospheric oxygen cannot be fully avoided, Fe(II) and S(-II) can react with oxygen, which leads to the production of H^+. We therefore suspect that the collected solution contained dissolved Fe(II), S(-II) or particulate Fe(II)-sulphides which became oxidised before analyses.

This interpretation is supported by the higher pH and higher Fe concentrations measured in the solution from sample Zee 103. During the squeezing of this sample, a thicker rubber stopper was used to close the bottle for a better protection of the solution against intrusion of atmospheric oxygen. Assuming that all measured Fe is in the form of Fe(II) and that alkalinity is only related to carbonate species, the solution of sample 103 is close to equilibrium with siderite. In contrast, Fe concentrations are lower in the other two samples and Fe could be removed from solution due to precipitation of iron (oxyhydr)oxides which was not directly noticed in the brown

bottles. The equilibrium concentration of ferrihydrite ($Fe(OH)_3$) in 0.5 M NaCl with a pH of 3.0 is about 0.24 mM, which is close to the Fe concentration in sample 104. The acidity produced upon oxidation of 2–3 mM of Fe(II) is sufficient to consume the alkalinity and reduce the pH to values around 3. Hence oxidation of Fe(II) in solutions from samples Zee 104 and Zee 101, when a thinner rubber stopper was applied, can explain the lower pH and lower dissolved Fe concentrations compared to the solution from sample 103. Furthermore, in none of the dilution experiments was an acidic pH detected, providing additional support to the conclusion that the acidic pH in samples Zee 104 and Zee 101 does not reflect the *in situ* pore water acidity but is caused by oxidation of dissolved Fe(II) after collection.

Calculated in situ pore water composition from results of dilution experiments

The composition of the *in situ* pore waters, which has been calculated from the results of the dilution experiment, confirms the strong seawater signature in the Rupel Clay pore water in Zeeland. Values for ionic strengths are in a similar range to that for pore waters collected by the squeezing method (Table 5). The charge imbalance of the individually analysed solutions was usually within the range of the progression of the analytical error, and the deviation from charge balance of the calculated composition of the pore waters was within a margin of ±10% when concentrations of all macro ions were available. The exception is the extrapolated pore water composition of Zee 101–14 obtained from dilutions with demineralised water. The excess in negative charge indicates that the extrapolation has led to an overestimation of Cl and SO_4 concentrations or an underestimation of the concentrations of the major cations in this sample. The calculated Cl concentrations of *in situ* pore waters vary between 73% and 103% of seawater concentration, with the exception of sample Zee 103A-01 (Table 5). This sample was collected from the top of core 103A and had most likely been subjected to desiccation and oxidation during the storage of the core. Oxidation is indicated by the presence of brown material along cracks. The solutions from sample Zee 103A-01 also differ significantly from others with respect to other parameters; in particular, the pH, with values above 10, is considerably higher. High pH values are a result of evaporation when CO_2 escapes from the concentrating solution. When evaporation proceeds, precipitates can form which do not readily dissolve when water is added and which might trap Ca, Mg or S. These precipitates include calcite, gypsum or silicates. When gypsum is the dominant Ca precipitate, the pH of the solution increases upon progressing evaporation. Due to the complexity of these reactions, the solution of sample Zee 103A-01 is not further considered when reconstructing the *in situ* pore water.

The concentrations of cations in the solutions from the dilution experiments differ among each other and from those in the pore water obtained by mechanical squeezing. Despite the variations, a few trends become apparent: the relative concentrations of K are higher while Mg concentrations, and with demineralised water also Ca, are lower in the *in situ* pore water, calculated from results of dilution experiments, than in the solutions obtained by mechanical squeezing. This trend was more pronounced when the dilution experiments were performed with $NaHCO_3$ than with demineralised water. Cation exchange might be the reason for the shift in cation concentrations during dilution. Addition of $NaHCO_3$ can displace the cation ratios in the solution, which results in Na adsorption coupled to the desorption of other cations such as K. Furthermore, dilution of a solution, which is in equilibrium with a cation exchanger, can lead to a redistribution of cations with different valency due to a relatively enhanced adsorption of bivalent over monovalent cations. Depletion of Mg and Ca combined with the release of K could therefore be ascribed to cation exchange reactions in the dilution experiments. A comprehensive discussion on the suitability of dilution experiments or squeezing techniques to determine *in situ* pore water composition of clay rocks is outside the scope of this study and can be found in Fernández et al. (2013). However, the effect of cation exchange on relative ion concentrations, and the ambiguity about the influence of processes with slow kinetics on the one hand and the ascertainment of the equilibrium state of fast processes on the other hand, can be considered a more severe source of bias than processes which might affect pore water composition during squeezing of clay samples.

The S concentrations of the solutions from the dilution experiments varied substantially between samples and for sample Zee 103–19a when demineralised water instead of $NaHCO_3$ was used in the dilution experiments. Furthermore, the S concentrations of the solutions from sample Zee 101–14 were about twice as high as in the solution squeezed out of core Zee 101. This indicates that the influence of processes producing or consuming dissolved S is very heterogeneous. In contrast to the other samples, the S concentrations in the dilutions of sample Zee 103–22 were all below the detection limit and, hence, the solution was depleted in S with respect to seawater. A possible explanation for the large variability of observed S concentrations is that elevated S concentrations were caused by pyrite oxidation which occurred only on a very localised scale during the storage of the core. This explanation is supported by visual inspection of the material during the slicing of the core (see Supplementary Material). In particular, parts of the core with higher sand content and brittle texture might have been more susceptible to oxygen penetration than parts with higher clay content and high plasticity. Progress of an oxidation front into Boom Clay has been investigated in the HADES (high-activity disposal experimental site) laboratory (De Craen et al., 2011). Decades of oxygen exposure altered the mineral composition only very close to the interface, while oxidation of pyrite was reflected in the pore water composition over a distance of 1 m.

Sample Zee 103–22 is a slice with high plasticity, and the low S concentrations might therefore reflect the pore water composition being unaffected by storage artefacts. In this case, the pore water in the *in situ* Rupel Clay is depleted in sulphate in comparison to seawater. Microbial sulphate reduction can account for the sulphate depletion which is also observed in the groundwater of the overlying Breda Formation.

Time evolution of solution composition in the dilution experiments

The goal of performing the dilution experiment over a period of one month was to evaluate the contribution of heterogeneous reactions with slower kinetics to changing the composition of the pore water. This includes, in particular, dissolution and precipitation of reactive minerals and microbial processes. A general trend in the dilution experiments with demineralised water and sample Zee 101-14 is that the ion concentrations are higher in solutions which were taken after a contact time of several days (Fig. 1). The concentrations of K and Na are higher after three days than after three hours but do not show a clear trend afterwards. In contrast, concentrations of Ca and Mg tend to increase over the whole period. The increase in Ca and Mg might be attributed to the dissolution of Ca/Mg carbonates possibly coupled to cation exchange reactions. That is, a part of the Ca released upon dissolution of calcite can become exchanged against Mg at the cation exchange complex. For a set of experiments, DIC concentrations were determined in the solutions at the end of the experiments (Zee 101–14, Zee 103A-19b and 103A-22) with demineralised water, and equilibrium speciation calculations have been performed. With sample Zee 101–14, final DIC concentrations increased with solid/solution, which supports the interpretation that carbonates dissolved during the experiments. None of the solutions reached equilibrium with calcite, and the saturation index ($SI = \log(IAP/K_{sp})$, where IAP is the ion activity product and K_{sp} is the solubility product) for the solutions from Zee 101–14 did not exceed −1.0. Saturation indices for the carbonates aragonite or dolomite were generally lower than those for calcite. This implies that the solutions remained corrosive with respect to Ca and Mg containing carbonates until the end of the experiments. The general increase in cation concentrations might also be caused by a delayed suspension of the material in demineralised water. Within three hours' reaction time, equilibrium with the cation exchange complex might not be achieved if clay particles are not completely dispersed. When the dispersion of clay aggregates continues over the next three days, additional cations might be released during the dilution experiment.

Presence of bicarbonate in the solution can mitigate the dissolution of carbonates or can even cause precipitation of carbonates when Ca and Mg are released from other sources, such as the exchange complex, and concentrations in solution exceed the solubility of carbonates. In experiments with sample Zee 101–14 and bicarbonate solution, Ca and Mg concentrations tend to decrease over time. The final DIC concentrations have not been analysed, but, assuming that the DIC concentrations were 10 mM, a positive SI for calcite indicates that the final solutions were oversaturated with respect to calcite. This supports the interpretation that precipitation of calcite has caused the decrease in Ca and, possibly via co-precipitation, also in Mg concentrations.

In experiments with sample Zee 103–22 (Fig. 2), the increase in Ca and Mg was very pronounced when demineralised water was added at the highest solid/solution ratio. Reaction of sample 103A-22 with demineralised water produced relatively high pH values (final pH was between 8.65 and 7.40 for lowest and highest solid/water ratios) which resulted in higher SI values than in the other experiments with demineralised water. Values for SI did not rise above −0.17. In experiments with Zee 103A-22 and bicarbonate solution, DIC concentrations were analysed. Despite the increase in Ca and Mg concentrations in experiments with bicarbonate solution, the decrease in DIC concentration in combination with a decrease in pH (from values of between 8.15 and 7.71 after three hours to final values between 7.90 and 7.39) suggests that carbonates precipitated. The SI of calcite in the final solutions was close to zero, indicating that dissolved Ca and carbonate concentrations are eventually controlled by calcite dissolution and precipitation. Possibly, the general trend of increasing concentrations of all macro ions is caused by retarded release of pore water or from sorption sites due to slow suspension of the clay aggregates. For Ca, and via co-precipitation for Mg, the release is counteracted by calcite precipitation in experiments with bicarbonate solution.

In all other experiments (Figs 3 and 4), the increase in Ca and Mg was only moderate, irrespective of whether demineralised water or bicarbonate solution was used in the experiments. Differences in the extent and the rates of Ca or Mg release between experiments with different samples can be attributed to different carbonate content or can be explained by inhibition of calcite dissolution by, for example, adsorption of phosphate (Berner, 1974). In some individual experiments with sample Zee 103A-19a, the Ca and Mg concentrations increased by a factor of two or more after 10 or 30 days' reaction time. This increase was only observed when bicarbonate solution was added, while, in general, the increase in Ca and Mg concentrations was higher with demineralised water. This pronounced increase in Ca and Mg took place in experiments with the lowest solid/solution ratio and also occurred in experiments with sample Zee 103A-19b with the lowest solid/solution ratio. In these experiments, the absolute Ca and Mg concentrations were lower than in the experiments with higher solid/solution ratios. The underlying reason for the exceptional abrupt release of Ca and Mg is enigmatic.

The time evolution of concentrations in experiments with sample Zee 103-01 is complex, and incongruent. Throughout the experiments, the pH values remained at levels between 9.5

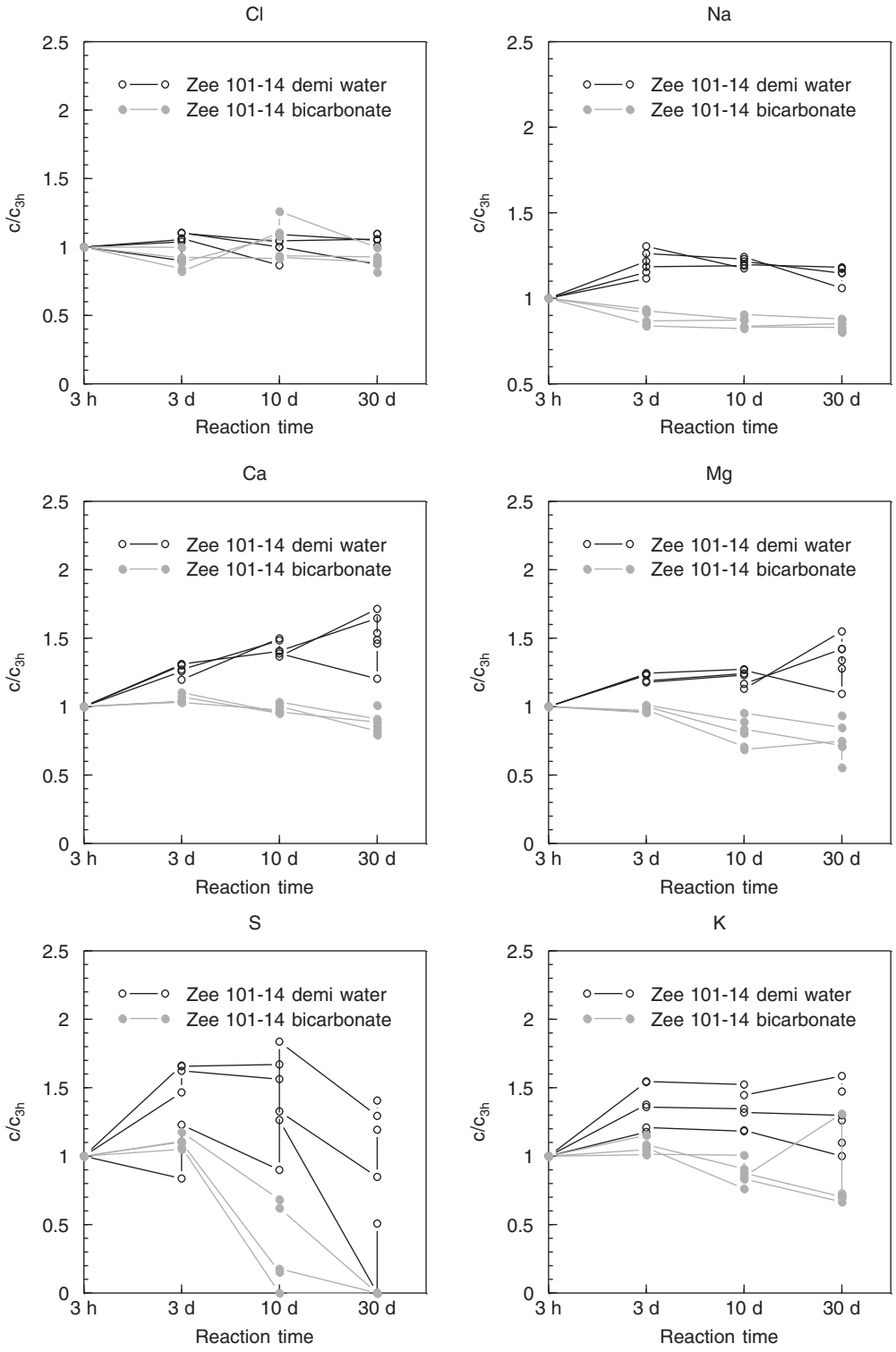

Fig. 1. Time evolution of the solution composition in the dilution experiments with sample Zee 101–14. Concentrations are normalised to the values determined in the first sampling moment after three hours' reaction time.

and 11.5 for the lowest and highest solid/solution ratio, respectively. The discussion of the underlying processes leading to the changes in solution composition for this sample falls outside the scope of this study as the alteration of the sample during storage is so severe that the processes during the dilution experiments have only very limited relevance for *in situ* conditions.

Sulphate most likely accounts for the majority of dissolved S in the samples, and in most cases its concentration showed higher dynamics compared to the time evolution of cation

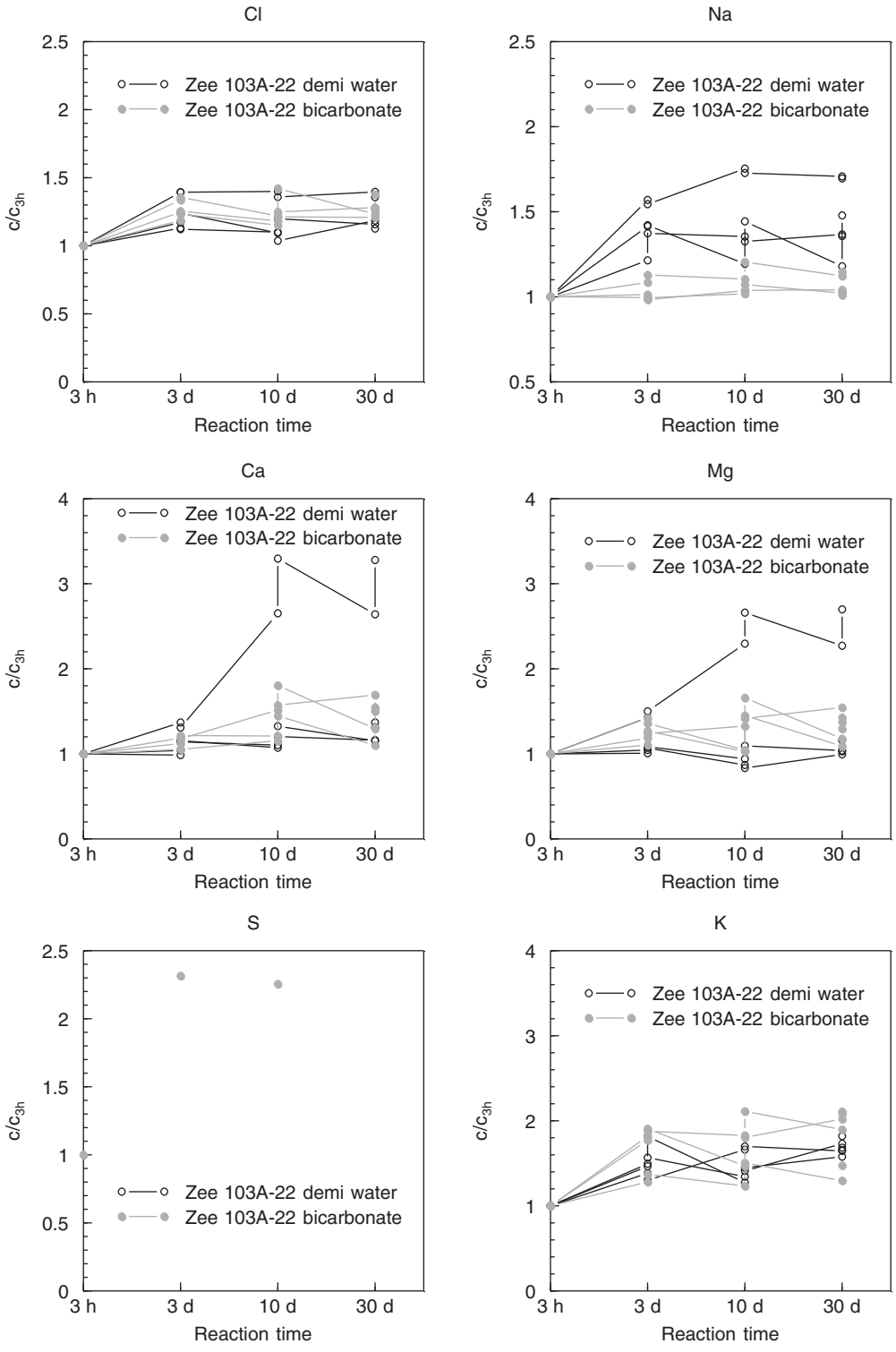

Fig. 2. Same as Figure 1, but for sample Zee 103A-22.

concentrations. This phenomenon is perplexing, as removal or release of sulphate has to be coupled to an increase or decrease in the concentrations of other ions in order to maintain charge balance. In sample Zee 103–19a and Zee 101–14, the common trend is that S concentrations increased in experiments with demineralised water during the first 10 days of reaction time. All solutions in the dilution experiments remained undersaturated with respect to gypsum, and therefore gypsum dissolution could be a source for the sulphate release. Afterwards, the concentrations tend to decrease. In experiments with bicarbonate, the S concentrations decrease and often reach values below detection limit. The difference in S increase between experiments

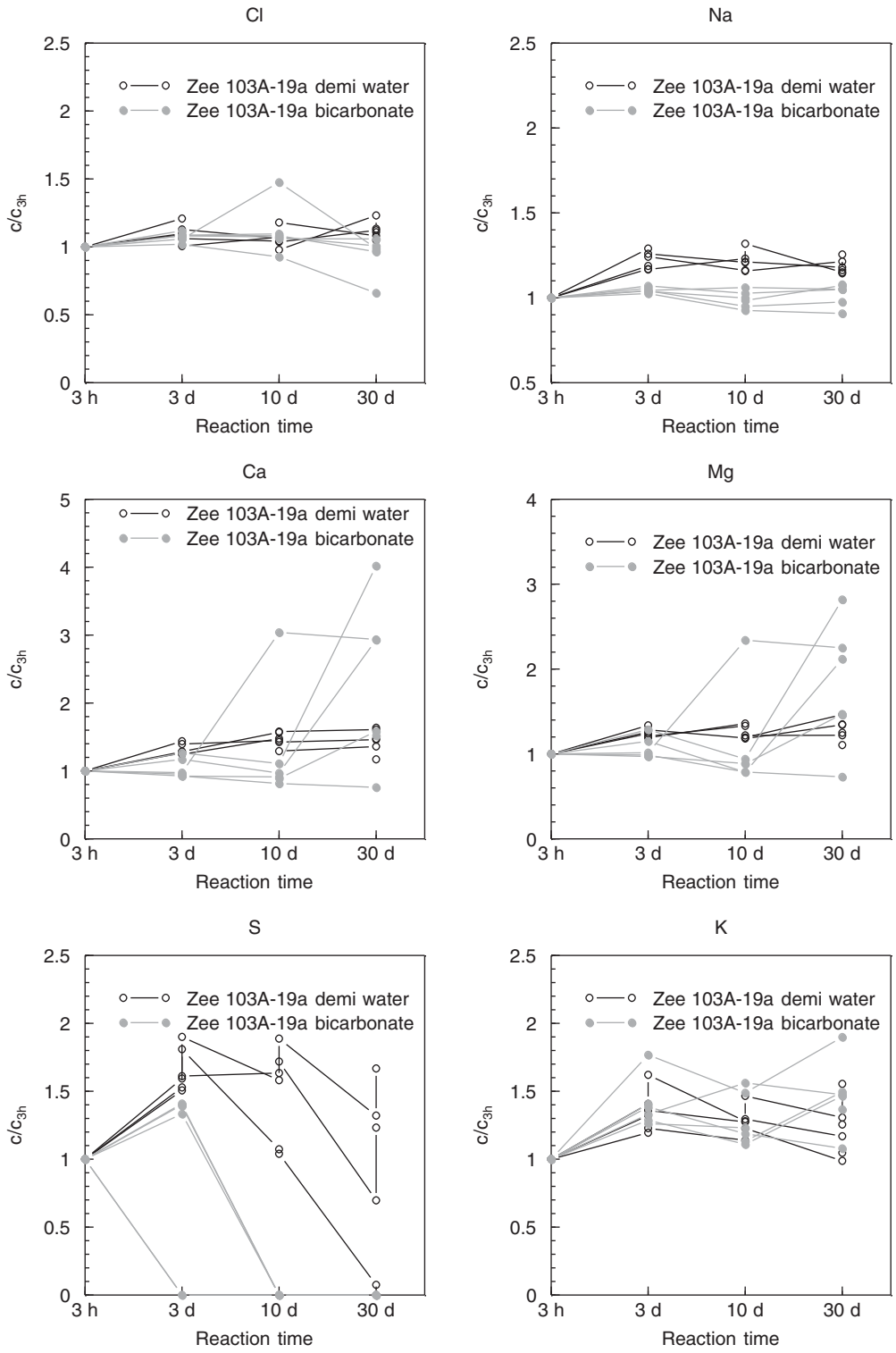

Fig. 3. Same as Figure 1, but for sample Zee 103A-19a.

with and without bicarbonate is enigmatic. In addition to the dissolution of sulphates, oxidation of sulphides or desorption of sulphate may account for an increase in dissolved S concentrations. However, any dissolution and precipitation reaction should also be reflected in the concentrations of the analysed cations and/or changes in pH values, but no systematic relationship was identified. Based on speciation calculations, a positive SI for barite was obtained, but Ba concentrations were generally low and it is unlikely that barite precipitation caused the removal of dissolved sulphate.

Biological activity might provide an explanation for the decrease in sulphate concentrations. A medium containing

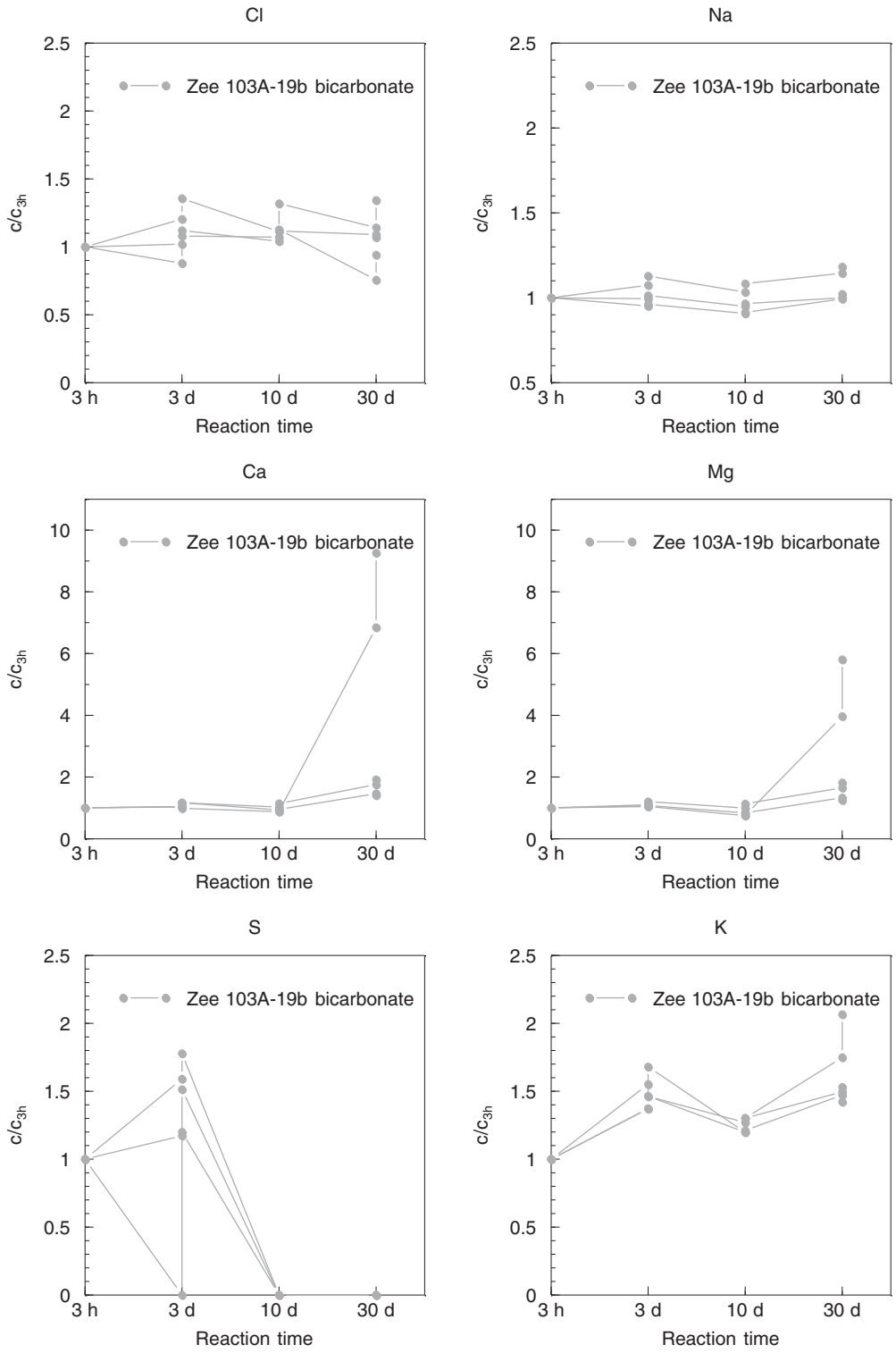

Fig. 4. Same as Figure 1, but for sample Zee 103A-19b.

bicarbonate might be more favourable for microorganisms. Sulphate-reducing bacteria have been identified in Boom Clay (Aerts et al., 2008) and they might become activated upon suspension. Suspension of the clays eliminates the space and transport limitations of microbial growth in Rupel Clay and might increase the bioavailability of organic matter. Also hydrogen gas, which entered the experiments during manipulations in the glove box, can serve as an electron donor. Without rigorous sterilisation, hydrogen gas used in diffusion experiments with Boom Clay from Belgium induced methane production by methanogenic organisms in the Boom Clay samples (Jacops et al., 2015) In our experiments, only traces (<0.12 mM)

of dissolved sulphide were detected at the end of the experiments, representing less than 1% of the initially dissolved S. The sulphide, produced by sulphate reduction, could react with iron phases forming iron sulphides. Unfortunately, our data do not provide information about the change in the composition of solids. Hence, further investigation is required to unravel the processes controlling the S dynamics in these experiments.

Sequential extractions

The difference between the sum of the sequentially extracted Fe and the Fe which is independently extracted by aqua regia is under 20%, with the exception of sample KB 101–26 (29.3%) and South-NL 19 (26.4%). Fe contents calculated from the sum of the individual extraction steps tend to be smaller than those of the independent aqua regia extractions. A systematic underestimation can be explained by loss of solids during the solid–solution separation steps between the different extractions. The content of total extractable Fe varies between 2.35 and 4.95 wt% (Fig. 5). The average concentration of extractable iron is 3.56 ± 0.61 wt%. The material from Limburg has, with 3.86 ± 0.55 wt%, a higher Fe concentration than the material from Zeeland, with 3.40 ± 0.60 wt%. However, the difference is not significant.

In the sequential extraction, the largest Fe fraction was extracted with aqua regia accounting for 68–81% in the samples from Zeeland and 57–72 % in the samples from Limburg. This fraction represents detrital Fe which is typically bound in silicates. The largest fraction of reactive Fe is extracted with concentrated HNO_3, which represents Fe in pyrite. In general, pyrite contents are higher in the Limburg samples than in samples from Zeeland. In particular, pyrite contents in the samples from the deeper part of Rupel Clay in Limburg are more than twice as high as in all other samples. This trend is in line with the S contents of the samples (see below). The differences in pyrite content between the upper and lower part of the Rupel Clay in Limburg and between those and the Rupel Clay from Zeeland are in agreement with the results of Koenen and Griffioen (2013). They found indications, based on S contents and results from X-ray diffraction (XRD) analysis, for higher pyrite contents in the deeper part of Rupel Clay in Limburg than in its upper part and compared to the core from Zeeland. However, the statistical analysis does not reveal a general geographical trend that Rupel Clay in the southeast of the Netherlands is generally richer in pyrite than Rupel Clay in the southwest.

Concentrations of adsorbed Fe, which is extracted with $MgCl_2$, is negligibly small, and Fe associated with organic matter, extracted with pyrophosphate, is only a minor fraction in all samples. The Fe fraction, which is extracted with 1 M HCl over four hours, varies between 0.11 and 0.39 wt% and does not show a significant difference between the different locations. This fraction might include carbonates, such as siderite, FeS or amorphous iron hydroxides, but also Fe which is released by partial dissolution from less reactive Fe phases. Determination of Fe(II) and Fe(III) in the HCl extracts with the ferrozine method revealed that practically all extracted Fe was in the form of Fe(III). Hence, most of the iron extracted with 1 M HCl originates from ferric iron (oxyhydr)oxides or from silicates whose partial dissolution cannot be completely suppressed under acidic conditions. This implies that FeS and Fe carbonates only account for a minor portion of reactive Fe in the samples.

Presence of iron (oxyhydr)oxides is also indicated by the results from the DCB extraction. Extraction with DCB targets crystalline iron (oxyhydr)oxides, and the amounts of Fe extracted with DCB are higher in samples from Zeeland compared to those from Limburg. Hence, the results from the sequential extractions indicate that Rupel Clay in Zeeland contains iron (oxyhydr)oxides. It cannot be excluded that a portion of the initially buried iron (oxyhydr)oxides have not been prone to sulphidisation during early diagenesis. Iron (oxyhydr)oxides have not yet been reported for Boom Clay, but nanocrystalline goethite has been identified in the reduced Callovian–Oxfordian clay formation of Bure, France (Kars et al., 2015). It is also possible that iron (oxyhydr)oxides have formed after burial upon the oxidation of pyrite. It cannot be fully excluded that the formation of iron (oxyhydr)oxides is an artefact of pyrite oxidation during core storage as discussed for the pore water sulphate concentrations. However, it is unlikely that iron (oxyhydr)oxides were solely formed during storage as relatively high contents of DCB-extractable Fe are also encountered in samples for which pore water sulphate concentrations are low (e.g. Zee 103A-22). No crystalline iron (oxyhydr)oxides were detected by XRD analysis of the samples from Zeeland and Limburg (Koenen and Griffioen, 2013). It is quite possible that the signal from the iron (oxyhydr)oxides is too small to be detected by XRD due to low contents and possibly due to low crystallinity or small particle size.

In addition to Fe, the concentrations of other elements in the extracts have been determined. Noticeably, Ca concentrations in the HCl extracts from samples from Limburg are, on average, about 10 times higher than those from Zeeland samples. Most of the Ca in these extracts originates from the dissolution of calcium carbonates, implying that the calcium carbonate content is significantly lower in the Zeeland samples than in those from Limburg. This finding is further supported by the C analyses (see below). Other significant differences between the locations include: (1) K concentrations in $MgCl_2$ extracts from Zeeland are about four times larger than those from Limburg, indicating the exchange complex of material from Zeeland contains relatively more K. (2) Concentrations of Al in HNO_3 extracts of samples from Zeeland are, on average more than twice as large as in extracts of samples from Limburg. This implies that the HNO_3 extract also dissolves Fe from clay minerals, but Fe from clay dissolution accounts for less than 10% of the extracted Fe, when assuming a molar Al/Fe ratio of about 0.16 in Dutch sedimentary clays (Huisman, 1998). High Al concentration in

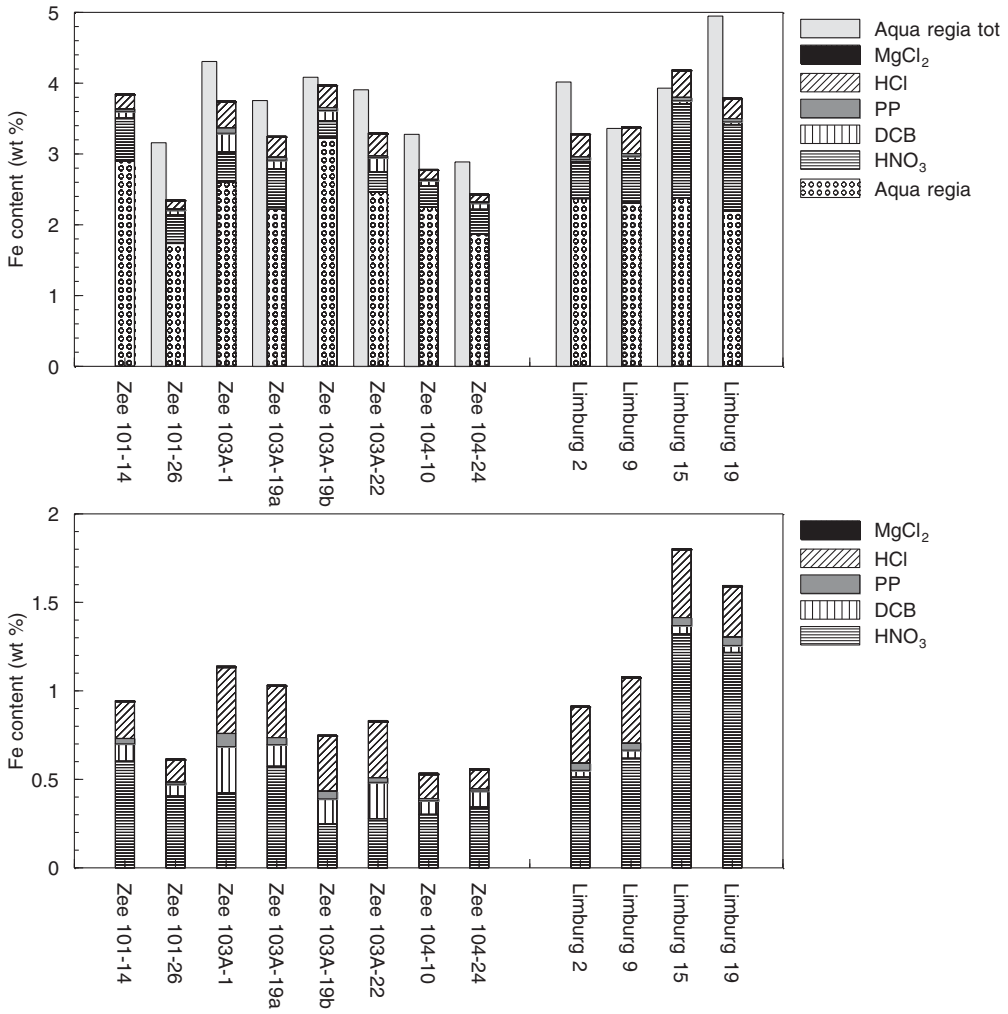

Fig. 5. Amount of iron extracted during the sequential extraction. $MgCl_2$ = 1 M magnesium chloride at pH 7; HCl = 1 M HCl, PP = 0.1 M sodium pyrophosphate at pH 10.4; DCB = Sodium citrate/dithionite solution buffered to a pH of 7.5 with $NaHCO_3$; Aqua regia tot = independent aqua regia extraction of all extractable Fe.

the HNO_3 extracts suggests that clay minerals in Rupel Clay in Zeeland are more prone to proton-promoted dissolution than those in the Rupel Clay in Limburg or that the Zeeland samples have a higher content of clay minerals. The latter is supported by the higher total Al contents in the Zeeland samples than in samples from the Rupel Clay in Zeeland (Koenen and Griffioen, 2013). (3) Mg concentrations in HNO_3 extracts are almost four times higher when collected from samples in Zeeland than from samples in Limburg. The Mg concentrations could be affected by the previous $MgCl_2$ extractions possibly inducing $MgSO_4$ precipitation and might not directly reflect the dissolution of initially present solids.

C, N, S contents

The S contents follow the trend in pyrite concentrations as inferred from the sequential extractions (Fig. 6), with the exception of sample Limburg 15, in which the S contents are significantly smaller than expected from the pyrite content, which was derived from sequential Fe extraction. The average S content in the samples from Limburg tends, with contents of 1.02 ± 0.44 wt%, to be higher than in Rupel Clay material from Zeeland (0.60 ± 0.15 wt%). Assuming that all S is bound in pyrite, these S contents correspond to average pyrite concentrations of 1.9 and 1.1 wt%, respectively. These values are in good agreement with those obtained from sequential extractions: yielding pyrite concentrations of 2.0 ± 0.9 wt% and 0.9 ± 0.3 wt% for samples from Zeeland and Limburg, respectively. Also the increase in pyrite concentrations with depth in the Rupel Clay in Limburg is similarly indicated by the S concentration profiles and the sequential extractions.

The difference in C contents before and after decalcification reflects the carbonate content of the samples. The difference in C content is most pronounced for samples from Limburg, while the change in C content upon decalcification is only marginal in samples from Zeeland (Table 6). For most samples, even higher C contents are obtained after decalcification. This observation can be explained by preferential loss of solids with

Table 6. Results of C,S and C,N analyses.

Sample name	C without decalcification (% wt)	S without decalcification (% wt)	C after decalcification (% wt)	N after decalcification (% wt)
Zee 101–14	0.48	0.87	0.41	0.042
Zee 101–26	0.41	0.48	0.24	0.031
Zee 103A-01	0.66	0.54	0.69	0.067
Zee 103A-19a	0.39	0.78	0.21	0.038
Zee 103A-19b	0.54	0.57	0.57	0.057
Zee 103A-22	0.62	0.50	0.65	0.069
Zee 104–10	0.37	0.47	0.44	0.048
Zee 104–24	0.41	0.61	0.43	0.046
Limburg 02	1.35	0.60	0.32	0.026
Limburg 09	1.39	0.82	0.61	0.042
Limburg 15	1.66	1.03	0.57	0.042
Limburg 19	1.73	1.63	1.40	0.081

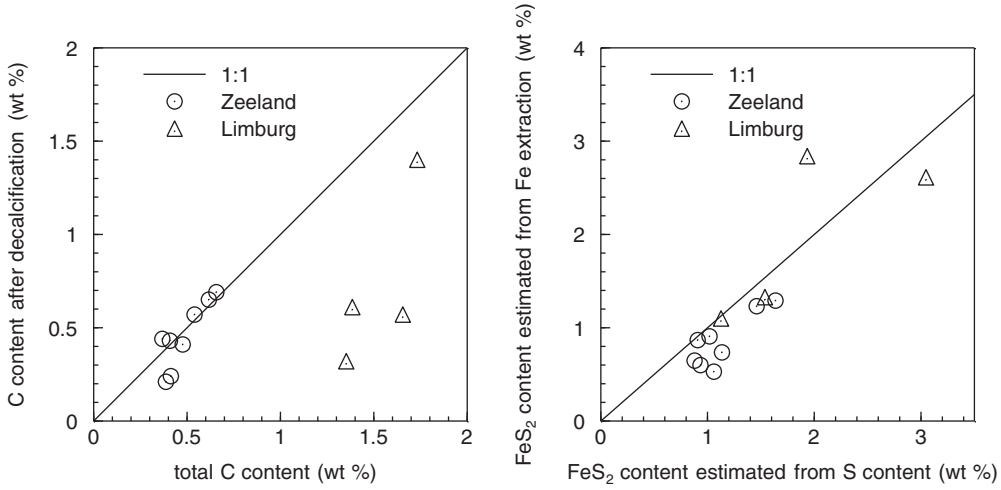

Fig. 6. Comparison of C contents in samples before and after decalcification (left panel) and FeS_2 contents estimated from S contents or based on the results from sequential Fe extraction (right panel).

low C content during the calcification procedure. Assuming that the change in C content is predominately due to the removal of calcium carbonate, Rupel Clay in Limburg contains 2.8–9.1 wt% $CaCO_3$ (based on stoichiometric conversion from C to $CaCO_3$ content). In contrast, the $CaCO_3$ content at the Zeeland location is smaller than 1.4 wt%, and in most samples the loss in C content upon decalcification indicates that some samples did not contain $CaCO_3$ at all. The difference in $CaCO_3$ content between the two locations is in line with the difference in Ca concentrations of 1 M HCl extracts (see above).

Lower $CaCO_3$ contents in Rupel Clay from Zeeland in comparison to Rupel Clay from Limburg are in line with the trend that Rupel Clay in the southwest has higher $CaCO_3$ contents than Rupel Clay in the southeast (Koenen and Griffioen, 2013). Aragonite and calcite were both detected by XRD analysis of a sample from the Zeeland core (Koenen and Griffioen, 2013) so that the absence of calcium carbonates in the core material, which is deduced from C analysis, is not confirmed by XRD analysis. The $CaCO_3$ values in the Rupel Clay samples from the drillings in Zeeland are below the lower limit of 1 wt% reported for Boom Clay in Belgium (De Craen et al., 2004). This is another indication for the alteration of the sediments by oxidation. As discussed previously, oxidation of pyrite generates acid which can be neutralised by carbonates, leading to dissolution of calcite and aragonite. It should be noted that most samples from the cores Zee 103 and Zee 104 still contain considerable amounts of pyrite while carbonate concentrations are very low or carbonates might even be absent. This implies that the acid potentially produced in these samples upon oxidation of the present pyrite cannot be neutralised by carbonate dissolution and can potentially lead to low pH values.

In all samples from Zeeland, the C content after decalcification, representing organic C, is below 0.7 wt%, which is also lower than the range (1–5 wt%) reported by De Craen et al. (2004) for the organic C content of Boom Clay. Decrease in organic C could also be a consequence of organic matter oxidation. However, comparison with the organic C content in Limburg samples does not suggest that, in contrast to $CaCO_3$, Rupel Clay in Zeeland is depleted in organic C.

Most of the N in the samples can be assumed to be organically bound, as the contribution of inorganic N, mostly in the form of adsorbed ammonium, to the total N content is only relevant in sediments with very low organic matter content (Müller, 1977). The C_{org}/N ratio is in the range of values reported for marine sediments (Müller, 1977; Ruttenberg and Goñi, 1997). The average value of the C_{org}/N ratios in samples from Limburg, 14.3 ± 4.7, is larger than the value for samples from Zeeland, 8.9 ± 2.4. A C_{org}/N ratio of 6.6 is traditionally assigned to living marine phytoplankton (Redfield, 1934; Fleming 1940). After dying off, the decomposition of the organic material leads to an increase in C/N ratio. The C_{org}/N ratio of freshly deposited, marine organic matter ranges around 10 (Rullkötter, 2006), matching the C_{org}/N ratios measured in the Zeeland samples. Larger C_{org}/N ratios, as obtained for the Rupel Clay samples from Limburg, might be a consequence of more pronounced diagenetic alterations or could indicate the input of a larger fraction of terrestrial organic matter with higher C_{org}/N ratios (Lamb, 2006). An east–west trend in C/N ratios of organic matter in Boom Clay in Belgium has been reported by Laenen (1997) and has been attributed to different input ratios of terrestrial and marine organic matter.

Cation exchange capacity

The average CEC of Rupel Clay material from the drillings in Zeeland is larger (18.5 ± 4.5 meq $(100\,g)^{-1}$) compared to the average CEC of Rupel Clay samples from Limburg (11.5 ± 1.3 meq $(100\,g)^{-1}$), when using the values based on the decrease in Cu solution determined by ICP-OES. The trend is in line with a larger fraction of swelling clay minerals in clay from Zeeland (45%) compared to that of Limburg (28.5–30.6%) based on XRD analysis (Koenen & Griffioen, 2013). In general, these values are in the reported range of 7–30 meq $(100\,g)^{-1}$ for the CEC of Boom Clay collected at different locations in Belgium (Honty, 2010).

The Cu concentration of the solids after reaction with Cu solution correlates with the decrease in Cu solution, but on average only about 75% were recovered in the solid phase. This discrepancy could be due to an underestimation of the Cu content of solids by TXRF, as part of the emitted X-ray fluorescence might become absorbed upon the passage through overlying solids. When the increase in concentration of cations in the Cu-containing solutions is used to determine the CEC, systematically higher values are obtained. This discrepancy is most pronounced in the samples from Limburg and can be attributed to the release of cations from other sources than the exchange complex. In particular, dissolution of calcium carbonates can lead to an overestimation of the CEC. The content of calcium carbonates is higher in the Rupel Clay in Limburg, which can explain the larger difference between the CEC values determined by Cu adsorption and release of cations.

Conclusions

The composition of pore waters retrieved by mechanical squeezing and the deduced composition of pore waters based on dilution experiments show a considerable variability. In dilution experiments, the major cation composition is shifted significantly due to cation exchange reactions. Hence, the composition of pore water, which is obtained by mechanical squeezing, provides a more direct indication of the *in situ* pore water if oxidation artefacts after the collection of the pore water are avoided. Despite the large variability between the composition of the different pore waters, some main trends can be identified which can be related to processes in Rupel Clay controlling the pore water composition in Zeeland.

The Rupel Clay in Zeeland separates saline groundwater above the formation from brackish groundwater, with about 40 times lower chloride concentrations, below the Rupel Clay. As a consequence, the pore waters have high electrolyte concentrations in the upper part of the Rupel Clay, with a decreasing trend towards its lower part. The pore water composition of samples from different depths reflects the effect of cation exchange on the progressive intrusion of marine cations. In particular, Na is depleted at the salinisation front and is exchanged against other cations such as Ca. When combining results from squeezing pore water and dilution experiments, indications are obtained that solubility equilibrium with calcite and the Fe carbonate siderite control Fe and Ca concentrations in the *in situ* pore water, although calcite concentrations can be very low and siderite is only a minor reactive Fe phase.

An important process affecting pore water composition and reactive mineral assemblage is the oxidation of pyrite in Rupel Clay from Zeeland. Groundwater overlying the Rupel Clay is depleted in sulphate, and pore water from samples, which were most likely not subject to oxidation artefacts during storage or pore water collection, also shows low sulphate concentrations. High sulphate concentrations in solutions obtained by squeezing Rupel Clay material or from dilution experiments with other samples are likely caused by pyrite oxidation during core storage and, in the case of some squeezed pore waters, after collection of the solution. Elevated sulphate concentrations are accompanied by increased Ca and Mg concentrations caused by carbonate dissolution and cation exchange, which are, in turn, initiated by acid production upon pyrite oxidation. As a

consequence, some pore waters are supersaturated with respect to gypsum.

Oxidation of pyrite can also explain differences in the content and occurrence of reactive solids. Rupel Clay in Zeeland contains ferric iron (oxyhydr)oxides which might be a product of pyrite oxidation. Furthermore, pyrite and carbonate contents in Rupel Clay in Zeeland are generally lower than in Limburg which could also be attributed to pyrite oxidation coupled to carbonate dissolution. These differences cannot be explained by storage artefacts alone but could be relicts of oxidation events in the past, possibly related to the erosion of Rupel Clay before deposition of the Breda Formation. No extractable carbonates were detected in several samples from Zeeland which still contain considerable amounts of pyrite. In these samples, acid neutralisation upon pyrite oxidation could be limited and pyrite oxidation could potentially lead to low pH values. Pyrite oxidation could be induced in Rupel Clay during construction and operation of a disposal facility for nuclear waste at the interface between the disposal facility and the host formation. Conversion of pyrite into iron (oxyhydr)oxides can have implications for the intensity of radionuclide migration and the underlying retardation mechanism. Pyrite is an important reductant for redox-sensitive radionuclides such as U or Se, and loss of pyrite might decrease the capacity of the clay to retard radionuclides if the reduced species has a lower mobility, as in the case of U (Bruggeman and Maes, 2010) and Se (Bruggeman et al. 2005). On the other hand, production of iron (oxyhydr)oxides might increase radionuclide retardation because iron (oxyhydr)oxides, produced by pyrite oxidation, usually have a large adsorption capacity and a high affinity for various radionuclides (Lack et al. 2002 and references therein).

This study also demonstrates the importance of minimising oxidation artefacts during core collection, storage and processing when targeting reactive minerals or pore water composition of unconsolidated clay-rich formations from anaerobic environments. In general, the core should be processed as soon as possible after collection. In addition to the measures performed in this study, storing at *in situ* temperature, vacuum sealing or storage under an inert atmosphere (N_2, Ar) could be helpful to preserve the original redox state. If sample manipulations or experiments cannot be performed in a glove box with an oxygen-free atmosphere, extra precautions should be taken to avoid contact between oxygen-sensitive pore water or solid material and atmospheric oxygen.

Acknowledgements

The research leading to these results has received funding from the Dutch research programme on geological disposal OPERA. OPERA is financed by the Dutch Ministry of Economic Affairs and the public limited liability company Elektriciteits-Produktiemaatschappij Zuid-Nederland (EPZ) and coordinated by COVRA. We thank SCK-CEN for performing the pore water collection by mechanical squeezing, and C. Bruggeman and N. Maes from SCK-CEN for advice and discussions related to this study.

Supplementary material

Supplementary material is available online at http://dx.doi.org/10.1017/njg.2016.23.

References

Aerts, S., ***Jacops, E.*** & ***Dewel, A.***, 2008. Microbial activity around the connecting gallery. SCK-CEN report ER-61.

Ammann, L., 2005. Determination of the cation exchange capacity of clays with copper complexes revisited. Clay Minerals 40: 441–453.

Appelo, C.A.J. & ***Postma, D.***, 2005. Geochemistry, groundwater and pollution, 2nd edn. A.A. Balkema Publishers (Leiden): 683 pp.

Berner, R.A., 1974. Dissolution kinetics of calcium carbonate in sea water; IV, Theory of calcite dissolution. American Journal of Science 274: 108–134.

Blount, C.W. & ***Dickson, F.***, 1973. Gypsum-anhydrite equilibria in systems $CaSO_4$-H_2O and $CaCO_4$-NaCl-H_2O. American Mineralogist 58: 323–331.

Brandse, W.P., ***van Rosmalen, G.M.*** & ***Brouwer, G.***, 1977. The influence of sodium chloride on the crystallization rate of gypsum. Journal of Inorganic and Nuclear Chemistry 39: 2007–2010.

Bruggeman, C. & ***Maes, N.***, 2010. Uptake of uranium(VI) by pyrite under Boom Clay conditions: influence of dissolved organic carbon. Environmental Science and Technology 44: 4210–4216.

Bruggeman, C., ***Maes, A.***, ***Vancluysen, J.*** & ***Vandenmussele, P.***, 2005. Selenite reduction in Boom clay: effect of FeS_2, clay minerals and dissolved organic matter. Environmental Pollution 137: 209–221.

Claff, S.R., ***Sullivan, L.A.***, ***Burton, E.D.*** & ***Bush, R.T.***, 2010. A sequential extraction procedure for acid sulfate soils: partitioning of iron. Geoderma 155: 224–230.

De Craen, M., ***Honty, M.***, ***Van Geet, M.***, ***Weetjens, E.***, ***Sillen, X.***, ***Wang, L.***, ***Jacques, D.*** & ***Martens, E.***, 2011. Overview of the oxidation around galleries in Boom Clay (Mol, Belgium) – status 2008. SCK-CEN report ER-189.

De Craen, M., ***Wang, L.***, ***Van Geet, M.*** & ***Moors, H.***, 2004. Geochemistry of Boom Clay pore water at the Mol site – status 2004. SCK-CEN report BSL-990.

De Craen, M., ***Wemaere, I.***, ***Labat, S.*** & ***Van Geet, M.***, 2006. Geochemical analyses of Boom Clay pore water and underlying aquifers in the Essen-1 borehole. SCK-CEN report ER-19.

Decleer, J., ***Viaene, W.*** & ***Vandenberghe, N.***, 1983. Relationships between chemical, physical and mineralogical characteristics of the Rupelian Boom Clay. Clay Minerals 18: 1–10.

Dohrmann, R., 2006. Cation exchange capacity methodology II: a modified silver–thiourea method. Applied Clay Science 34: 38–46.

Donisa, C., 2007. Combination of different extractants to assess binding forms of some elements in soil profiles. Communications in Soil Science and Plant Analysis 39: 177–186.

Fernández, A., ***Sánchez-Ledesma, D.***, ***Tournassat, C.***, ***Melón, A.***, ***González, A.***, ***Gaucher, E.*** & ***Vinsot, C.***, 2013. Applying squeezing technique to clayrocks:

lessons learned from experiments at Mont Terri Rock Laboratory. Informes Técnicos Ciemat report 1300.

Fleming, R.H., 1940. The composition of plankton and units for reporting population and production. Sixth Pacific Science Congress, Berkeley, CA, USA. Conference proceedings 3: 535–540.

Gleyzes, C., 2002. Fractionation studies of trace elements in contaminated soils and sediments: a review of sequential extraction procedures. Trends in Analytical Chemistry 21: 451–467.

Griffioen, J., 2015. The composition of deep groundwater in the Netherlands in relation to disposal of radioactive waste. COVRA report OPERA-PU-TNO521-2.

Griffioen, J., ***Stuurman, R.*** & ***Verweij, H.***, 2016. The composition of groundwater in Palaeogene and older formations in the Netherlands. A synthesis. Netherlands Journal of Geosciences, this issue.

He, S., ***Oddo, J.E.*** & ***Tomson, M.B.***, 1994. The nucleation kinetics of calcium sulfate dihydrate in NaCl solutions up to 6 m and 90°C. Journal of Colloid Interface Science 162: 297–303.

Holland, H. D., 1984. The chemical evolution of the atmosphere and oceans. Princeton University Press (Princeton, NJ): 582 pp.

Honty, M., 2010. CEC of the Boom Clay – a review. SCK-CEN report ER-134.

Honty, M. & ***De Craen, M.***, 2009. Mineralogy of the Boom Clay in the Essen-1 borehole. SCK-CEN report ER-87.

Honty, M. & ***De Craen, M.***, 2012. Boom Clay mineralogy – qualitative and quantitative aspects. SCK-CEN report ER-194.

Huerta Diaz, M.A., 1990. A quantitative method for determination of trace metal concentrations in sedimentary pyrite. Marine Chemistry 29: 119–144.

Huisman, D.J., 1998. Geochemical characterization of subsurface sediments in the Netherlands. PhD Thesis. Wageningen University (Wageningen).

Jacops, E., ***Wouters, K.***, ***Volckaert, G.***, ***Moors, H.***, ***Maes, N.***, ***Bruggeman, C.***, ***Swennen, R.*** & ***Littke, R.***, 2015. Measuring the effective diffusion coefficient of dissolved hydrogen in saturated Boom Clay. Applied Geochemistry 61: 175–184.

Kars, M., ***Lerouge, C.***, ***Grangeon, S.***, ***Aubourg, C.***, ***Tournassat, C.***, ***Made, B.*** & ***Claret, F.***, 2015. Identification of nanocrystalline goethite in reduced clay formations: application to the Callovian-Oxfordian formation of Bure (France). American Mineralogy 100: 1544–1553.

Koenen, M. & ***Griffioen, J.***, 2013. Mineralogical and geochemical characterization of the Boom Clay in the Netherlands. COVRA report OPERA-PU-5-2-1-TNO-1.

Koenen, M. & ***Griffioen, J.***, 2016. Characterisation of the geochemical heterogeneity of the Rupel Clay Member in the Netherlands. Netherlands Journal of Geosciences, this issue.

Lack, J.G., ***Chaudhuri, S.K.***, ***Kelly, S.D.***, ***Kemner, K.M.***, ***O'Connor, S.M.*** & ***Coates, J.D.***, 2002. Immobilization of radionuclides and heavy metals through anaerobic bio-oxidation of Fe(II). Applied and Environmental Microbiology 68: 2704–2710.

Laenen, B., 1997. The geochemical signature of relative sea-level cycles recognized in the Boom Clay. PhD Thesis. Katholike Universiteit Leuven (Leuven).

Lamb, A.L., 2006. A review of coastal palaeoclimate and relative sea-level reconstructions using δ^{13}C and C/N ratios in organic material. Earth-Science Reviews 75: 29–57.

Larner, B.L., 2006. Comparative study of optimised BCR sequential extraction scheme and acid leaching of elements in the certified reference material NIST 2711. Analytica Chimica Acta 556: 444–449.

Mossop, K.F., 2003. Comparison of original and modified BCR sequential extraction procedures for the fractionation of copper, iron, lead, manganese and zinc in soils and sediments. Analytica Chimica Acta 478: 111–118.

Müller, P.J., 1977. CN ratios in Pacific deep-sea sediments: effect of inorganic ammonium and organic nitrogen compounds sorbed by clays. Geochimica et Cosmochimica Acta 41: 765–776.

Parkhurst, D.L., & ***Appelo, C.A.J.***, 2013. Description of input and examples for PHREEQC version 3 – a computer program for speciation, batch-reaction, one-dimensional transport, and inverse geochemical calculations. US Geological Survey Techniques and Methods, book 6, ch. A43, 497 pp., available at http://pubs.usgs.gov/tm/06/a43/.

Redfield, A.C. 1934. On the proportions of organic derivatives in sea water and their relation to the composition of plankton. James Johnstone Memorial Volume. University Press of Liverpool (Liverpool): 177–192.

Rijkers, R.H.B., ***Huisman, D.J.***, ***de Lange, G.***, ***Weijers, J.P.*** & ***Witmans-Parker, N.***, 1998. Inventarisatie geomechanische, geochemische en geohydrologische eigenschappen van Teriaire kleipakketten – CAR Fase II. COVRA report TNO NITG 98-90 B.

Rullkötter, J., 2006. Organic matter: the driving force for early diagenesis. *In*: ***Schulz, H.*** & ***Zabel, M.*** (eds): Marine chemistry. Springer Berlin (Heidelberg): 125–168.

Ruttenberg, K.C. & ***Goñi, M.A.***, 1997. Phosphorus distribution, C:N:P ratios, and δ^{13}Coc in arctic, temperate, and tropical coastal sediments: tools for characterizing bulk sedimentary organic matter. Marine Geology 139: 123–145.

Scouller, R.C., 2006. Evaluation of geochemical methods for discrimination of metal contamination in Antarctic marine sediments: a case study from Casey Station. Chemosphere 65: 294–309.

Stuyfzand, P.J., 2008. Base exchange indices as indicators of salinization or freshening of (coastal) aquifers. 20th Salt Water Intrusion Meeting, 23–27 June 2008, Naples, FL, USA, 281–284. Conference proceedings.

Tessier, A., 1979. Sequential extraction procedure for the speciation of particulate trace metals. Analytical Chemistry 51: 844–851.

TNO, 2003. Explanation to Map Sheets Xl and XII Middelburg-Breskens and Roosendaal-Terneuzen, Geological Atlas of the Subsurface of the Netherlands, Netherlands lnstitute ofApplied Geoscience TNO - National Geological Survey, Utrecht 2003.

TNO, n.d. *Subsurface models*. Available from https://www.dinoloket.nl/en/subsurface-models.[26 May 2015]

Tournassat, C. & ***Steefel, C.I.***, 2015. Ionic transport in nano-porous clays with consideration of electrostatic effects. Reviews in Mineralogy and Geochemistry 80: 287–329.

Vandenberghe, N., 1974. Een sedimentologische studie van de Booms Klei. PhD Thesis. Katholieke Universiteit Leuven (Leuven).

Vandenberghe, N., 1978. Sedimentology of the Boom Clay (Rupelian) in Belgium. Verhandeling Koninklijke Academie voor Wetenschappen, Letteren en Schone Kunsten van Blegië, Klasse Wetenschappen XL.

Viollier, E., ***Inglett, P.W.***, ***Hunter, K.***, ***Roychoudhury, A.N.*** & ***Van Cappellen, P.***, 2000. The ferrozine method revisited: Fe(II)/Fe(III) determination in natural waters. Applied Geochemistry 15: 785–790.

Zeelmaekers, E., 2011. Computerized qualitative and quantitative clay mineralogy. PhD Thesis. Katholike Universiteit Leuven (Leuven).